THE JOURNAL OF BIOLOGICAL CHEMISTRY VOL. 290, NO. 37, pp. 22370–22384, September 11, 2015

Protein Kinase CK2 Interacts at the Neuromuscular Synapse with Rapsyn, Rac1, 14-3-3γ, and Dok-7 Proteins and Phosphorylates the Latter Two*

Received for publication, February 26, 2015, and in revised form, July 8, 2015 Published, JBC Papers in Press, July 21, 2015, DOI 10.1074/jbc.M115.647610

Dustin Herrmann[1], **Marion Straubinger**[1], **and Said Hashemolhosseini**[2]

From the Institut für Biochemie, Friedrich-Alexander Universität Erlangen-Nürnberg, Fahrstrasse 17, D-91054 Erlangen, Germany

Background: Knowledge about the role of the protein kinase CK2 at neuromuscular synapses is limited.
Results: CK2 binds different postsynaptic proteins, Rapsyn, Rac1, 14-3-3γ, and Dok-7, and phosphorylates two of them. Phosphomimetic Dok-7 mutants improve neurotransmitter receptor aggregation.
Conclusion: Phosphorylation of synaptic proteins by CK2 appears important for postsynaptic neurotransmitter receptor aggregation.
Significance: Better understanding of signaling cascades involved in aggregation of neurotransmitter receptors offers possibilities for therapeutical intervention.

Previously, we demonstrated that the protein kinase CK2 associates with and phosphorylates the receptor tyrosine kinase MuSK (muscle specific receptor tyrosine kinase) at the neuromuscular junction (NMJ), thereby preventing fragmentation of the NMJs (Cheusova, T., Khan, M. A., Schubert, S. W., Gavin, A. C., Buchou, T., Jacob, G., Sticht, H., Allende, J., Boldyreff, B., Brenner, H. R., and Hashemolhosseini, S. (2006) *Genes Dev.* 20, 1800–1816). Here, we asked whether CK2 interacts with other proteins involved in processes at the NMJ, which would be consistent with the previous observation that CK2 appears enriched at the NMJ. We identified the following proteins to interact with protein kinase CK2: (*a*) the α and β subunits of the nicotinic acetylcholine receptors with weak interaction, (*b*) dishevelled (Dsh), and (*c*) another four proteins, Rapsyn, Rac1, 14-3-3γ, and Dok-7, with strong interaction. CK2 phosphorylated 14-3-3γ at serine residue 235 and Dok-7 at several serine residues but does not phosphorylate Rapsyn or Rac1. Furthermore, phosphomimetic Dok-7 mutants aggregated nicotinic acetylcholine receptors in C2C12 myotubes with significantly higher frequency than wild type Dok-7. Additionally, we mapped the interacting epitopes of all four binding partners to CK2 and thereby gained insights into the potential role of the CK2/Rapsyn interaction.

Earlier, we reported that protein kinase CK2 (formerly called casein kinase 2) interacts and co-localizes with the receptor tyrosine kinase muscle specific receptor tyrosine kinase (MuSK)[3] at the neuromuscular junction (NMJ) (1). MuSK binding partners are of fundamental interest at this synapse because MuSK activation is known to be responsible for the aggregation of AChRs, which represents a hallmark of postsynaptic apparatus formation (2). Protein kinase CK2 is a ubiquitously expressed serine/threonine kinase composed of four subunits: two catalytically active α and two regulatory β subunits (3). Earlier, we observed CK2-mediated phosphorylation of serine residues 680 and 697 within the cytosolic kinase domain of MuSK *in vitro* (1). MuSK activity was not changed, but AChR stability appeared to decrease in the presence of CK2 inhibitors (1). Moreover, muscle-specific CK2β knock-out mice develop a myasthenic phenotype likely due to impaired muscle end plate structure and function (1). Although CK2 is known to phosphorylate hundreds of proteins (3), up to now no more targets have been reported in a neuromuscular context.

Here, we asked whether protein kinase CK2, previously observed to be enriched at NMJs (1), might interact with other synaptic proteins and whether CK2 might be involved in their phosphorylation. We identified Rapsyn, Rac1, 14-3-3γ, and Dok-7 as binding partners of protein kinase CK2.

The cytosolic scaffold protein Rapsyn mediates the aggregation of AChRs in stoichiometric fashion (4–6). It is known to be composed of seven amino-terminally localized tetratricopeptide repeats (TPRs) and a carboxyl-terminally localized coiled coil and RING domain (7), respectively. Rapsyn perfectly matches the localization of AChRs at NMJs (8, 9).

It is known that AChR clustering in myotubes also depends on the small GTPases Rac1 and Cdc42 (10). Previous data show that for AChR clustering the activation of Rac1 and Cdc42 is required and that this activation is most likely controlled via reorganization of the actin cytoskeleton (11).

The 14-3-3 proteins comprise several isoforms and are known to regulate cellular processes by binding signal transduction proteins. Forced expression of 14-3-3γ in myotubes or muscle fibers induces both the specific repression of synaptic gene transcription and morphological perturbations of the NMJ (12).

Dok-7 is the only member of the Dok family of cytoplasmic molecules that induces the aneural activation of MuSK and the

* This work was supported by Deutsche Forschungsgemeinschaft Grants HA 3309/1-1 to 1-3) and by the Interdisciplinary Centre for Clinical Research at the University Hospital of the University of Erlangen-Nuremberg (Grant E2) (both to S. H.). The authors declare that they have no conflicts of interest with the contents of this article.
[1] Both authors contributed equally to this work.
[2] To whom correspondence should be addressed. Tel.: 49-9131-85-24634; Fax: 49-9131-85-22484; E-mail: said.hashemolhosseini@fau.de.
[3] The abbreviations used are: MuSK, muscle specific receptor tyrosine kinase; NMJ, neuromuscular junction; AChR, nicotinic acetylcholine receptor; Dsh, dishevelled; TPR, tetratricopeptide repeat; PH, pleckstrin homology; aa, amino acids; NLS, nuclear localization signal; BTX, bungarotoxin.

subsequent clustering of AChRs in cultured myotubes (13). Like the other members of the Dok family, Dok-7 is composed of a pleckstrin homology (PH) domain and phosphotyrosine binding domain in its amino-terminal portion and Src homology 2 domain target motifs in its carboxyl-terminal region (13).

To further characterize the interaction of CK2 with these key players at the NMJ, we identified the epitopes within Rapsyn, Rac1, 14-3-3γ, and Dok-7 that interact with the protein kinase CK2. Additionally, CK2 even phosphorylated 14-3-3γ and Dok-7 but not Rac1 and Rapsyn *in vitro*. For Rapsyn, we predicted serine 224 as a potential CK2 target *in vivo*, and we demonstrated that a phosphomimetic Rapsyn mutant was able to bind CK2 with higher affinity. Serine residue 235 of 14-3-3γ was identified to be a CK2 phosphorylation target site. Tellingly, Dok-7 was strongly phosphorylated at several serine residues by CK2. Dok-7 phosphomimetic mutants improved AChR aggregation on C2C12 myotubes.

Experimental Procedures

Plasmid Constructs—For GST pulldown experiments and co-immunoprecipitation studies, the coding sequences of various mouse genes were cloned into pcDNA3–6HA to generate the respective expression plasmids. As template, cDNA of mouse hind limb muscle or C2C12 myotubes was used to PCR-amplify the different DNA fragments with appropriate primer pairs. Expression plasmids for MuSK were described previously (1). The generation of full-length CK2α and CK2β fused to GST using the vector pGEX-KG and all other CK2 expression plasmids have been described (1).

For epitope mapping studies, different epitopes of mouse Dok-7, 14-3-3γ, Rapsyn, and Rac1 were amplified by PCR and cloned into pGEX-KG to generate GST fusions, and the recombinant GST fusion proteins were purified from *Escherichia coli*. For generating mutants (carboxyl-terminal truncations) of Dok-7, 14-3-3γ, Rapsyn, and Rac1, appropriate primers were used. For *in vitro* CK2 phosphorylation studies, different PCR-amplified epitopes of mouse Dok-7 and 14-3-3γ were fused to GST using pGEX-KG and the restriction sites BamHI and HindIII or BamHI and XhoI.

Substitutions of serine or threonine residues by alanines, aspartates, or glutamates were introduced into the full-length Dok-7, 14-3-3γ, or Rapsyn plasmids after cloning into pGEX-KG or pcDNA3-6HA and in the Dok-7 fragments aa238–282 and aa283–347 after insertion into pGEX-KG using the QuikChange XL site-directed mutagenesis kit (Stratagene) or the Q5® site-directed mutagenesis kit (New England Biolabs) following the manufacturers' protocols. All mutations were verified by sequencing (LGC Genomics) after each cloning step. Phosphorylation site predictions were conducted using KinasePhos 2.0 (14).

Tissue Culture, Transfection, Lysate Preparation, and Western Blotting—HEK293 cells were maintained in Dulbecco's modified Eagle's medium (DMEM) containing 10% (v/v) fetal calf serum (FCS; Invitrogen). HEK293 cells were transfected using PEI (Sigma-Aldrich). 10-cm plates were transfected with 10 μg of vector and 31 μl of 1× PEI for 12–24 h. Cell lysates were prepared 48 h after transfection. Cells were washed twice with cold 1× PBS and lysed in lysis buffer containing 50 mM HEPES (pH 7.5), 10% glycerol, 150 mM NaCl, 1% Triton X-100, 1.5 mM $MgCl_2$, 1 mM EGTA (pH 8), and a mixture of proteinase inhibitors (1 mM PMSF and 10 μg/μl aprotinin and leupeptin).

For detection of proteins in Western blot analysis, monoclonal antibodies directed against the myc epitope (Cell Signaling Technology), the hemagglutinin epitope (Santa Cruz Biotechnology), CK2β (Olaf-Georg Issinger, Odense, Denmark), Dok-7 (Santa Cruz Biotechnology), and GAPDH (Santa Cruz Biotechnology) served as primary antibodies, and anti-mouse or -rabbit Ig-coupled horseradish peroxidase (Cell Signaling Technology) was used as secondary antibodies. For detection, the ECL detection system (Amersham Biosciences) was used.

Gastrocnemius and soleus muscles were dissected from wild type mice, dissolved in 3 ml of lysis buffer (1 M HEPES (pH 7.9), 1 M KCl, 0.5 M EDTA, 1 M DTT, and 10 μg/ml aprotinin and leupeptin) supplemented with Nonidet P-40, and homogenized on ice. 250 μl of 5 M NaCl were added, the solution was rotated for 15 min at 4 °C and centrifuged, and the supernatant was frozen in liquid nitrogen and stored at −80 °C.

Immunoprecipitation and GST Pulldowns—For each extract of transiently transfected HEK293 cells, the expression level of the desired protein was analyzed by Western blotting. Then, for co-immunoprecipitation studies, 1 μl of a monoclonal antibody against the myc epitope was added, and the samples were incubated overnight at 4 °C under constant rotation. Next, 20 μl of PBS-equilibrated protein A-Sepharose CL-4B beads (Amersham Biosciences) were added, and incubation continued for another 2–4 h at 4 °C. After washing the beads in 50 mM HEPES (pH 7.5), 150 mM NaCl, 1 mM EDTA, 10% glycerol, 1 mM PMSF, 10 μg/ml leupeptin, and 10 μg/ml aprotinin, the precipitated proteins were analyzed by SDS-PAGE and Western blotting.

For GST pulldowns, BL21 bacteria were transformed with the respective constructs, grown in 200-ml cultures at 37 °C until A_{600} was between 0.4 and 0.6, and induced by 1 mM isopropyl 1-thio-β-D-galactopyranoside for 4–6 h at 37 °C to express the GST fusion proteins. Bacteria were collected by centrifugation, incubated in sonication buffer (50 mM NaH_2PO_4, 300 mM NaCl, 10 μg/ml leupeptin, 10 μg/ml aprotinin, 1 μl/ml Triton X-100, 10 μg/ml DNase I, and 15 units/μl Lysozyme) at 4 °C for 30 min, lysed by sonication for a total time of 1 min, and centrifuged. The supernatants containing the GST fusion proteins were supplemented with 30 μl of equilibrated glutathione beads and incubated under constant rotation at 4 °C for 2–12 h. After washing three times with washing buffer (4.3 mM Na_2HPO_4, 1.47 mM KH_2PO_4, 137 mM NaCl, and 2.7 mM KCl), an aliquot of the beads, now carrying the GST fusion protein, was incubated with the extract from HEK293 cells expressing the desired protein after transient transfection. After washing the beads another three times with washing buffer containing 137 mM NaCl or 20 mM NaCl, proteins bound to the beads were analyzed by SDS-PAGE and Western blotting.

For purification of recombinant Dok-7- and Rapsyn-GST fusion proteins, a different protocol was used. The bacterial pellet was resuspended in ice-cold STE buffer (10 mM Tris-HCl (pH 8), 1 mM EDTA, and 150 mM NaCl). Then, after adding 0.1 mg/ml lysozyme, the bacterial pellet was incubated on ice

for 15 min, supplemented with 10 mM DTT and 1.2% Sarkosyl, and sonicated for a total time of 1 min. After centrifugation, the supernatant was diluted with STE buffer so that the concentration of Sarkosyl reached 0.7%, and Triton X-100 was added at a concentration of 2%. The lysate was incubated for 1 h on ice, then supplemented with PBS-equilibrated glutathione beads, and incubated with agitation at 4 °C for 2–12 h. Finally, the beads were washed three times with cold PBS.

[γ-^{32}P]ATP Incorporation Assay—Recombinant purified full-length proteins or the indicated domains of CK2-interacting proteins were phosphorylated *in vitro* by CK2α (20 pmol; Kinase Logistics ApS, Denmark) alone or together with CK2β (20 pmol; Kinase Logistics ApS) in 50 mM Tris-HCl (pH 8), 10 mM MgCl2, and 1 mM DTT. After addition of [γ-^{32}P]ATP, samples were incubated for 30 min at 30 °C; the reactions were stopped by addition of Laemmli buffer, and samples were analyzed by SDS-PAGE and autoradiography. As a positive control, CK2 activity was analyzed using a previously described synthetic peptide substrate (RRRDDDSDDD) (1). A 0.2 mM concentration of the peptide was incubated in 50 mM HEPES buffer (pH 7.5), 10 mM $MgCl_2$, 0.5 mM DTT, 50 mM NaCl, and 50 μM [γ-^{32}P]ATP (specific activity, 3500–7800 cpm/pmol) with recombinant CK2α from *Xenopus laevis* for 30 min (verification by SDS-PAGE) at 30 °C. The verification of the phosphorylation experiment by SDS-PAGE required [γ-^{32}P]ATP with a specific activity of 20,000 cpm/pmol. The reaction was spotted onto P81 phosphocellulose paper and washed three times in ice-cold 75 mM H_3PO_4. Paper-associated radioactivity was measured by scintillation counting. Control values obtained in assays without added enzyme were subtracted. For each peptide, the experiment was performed three times independently. For verification, reactions were analyzed by 14% SDS-PAGE. Radioactive bands were detected on a Molecular Imager FX apparatus (Bio-Rad).

Immunohistochemistry—For immunohistochemical analysis, musculus gastrocnemius cross-sections were rinsed with PBS, fixed with 2% paraformaldehyde for 5 min, and permeabilized for 5 min with PBS supplemented with 0.1% Triton X-100 for 5 min. Then, sections were blocked in blocking solution (10% FCS and 1% BSA in PBS) for 1–2 h. For the monoclonal mouse α-CK2β (a gift from Olaf-Georg Issinger, Odense, Denmark), blocking was performed with a 1:40 dilution of M.O.M reagent (Vector Laboratories) under equivalent conditions to reduce unspecific binding. Thereafter, the sections were stained with the respective antibodies (dissolved in the blocking solution) at 4 °C overnight. For detection, primary antibodies α-CK2β (gift from Olaf-Georg Issinger, Odense, Denmark), α-Dok-7 (Santa Cruz Biotechnology), α-14-3-3γ (Santa Cruz Biotechnology), α-Rapsyn (Acris), and α-Rac1 (Millipore) were combined with secondary antibodies α-Alexa Fluor 488 (Molecular Probes) and α-Cy3 (Dianova). Secondary antibodies were applied for 2 h at room temperature. Subsequently, sections were washed six times for 5 min in PBS and embedded with Mowiol.

Immunocytochemistry and Analysis of Dok-7-mediated Clustering—Electroporation with the Nucleofector™ kit V (Lonza) was used for transfection of C2C12 myoblasts. The cells were cultured on a 10-cm plate until confluence reached 60%, washed with sterile PBS, trypsinized, and harvested by centrifugation for 10 min at 90 × *g*. The pellet was resuspended in 100 μl of Nucleofector reagent, and the total amount of plasmid was added (4 μg total; 3.5 μg of expression construct + 0.5 μg of pCMV GFP-NLS). The cells were then electroporated in a Nucleofector cuvette, diluted in 15 ml of proliferation medium (DMEM, 20% FCS, and 1% penicillin/streptomycin), and distributed to 3.5-cm plates that had previously been coated with 25 μl of Matrigel. After 24 h, the medium was changed to differentiation medium (DMEM, 1% penicillin/streptomycin, and 5% horse serum). Prior to staining, C2C12 cells were fixed with cold 2% paraformaldehyde for 30 min. To visualize AChR clusters, rhodamine- or Alexa Fluor 647-coupled α-bungarotoxin (α-BTX) was applied at a 1:2,500 dilution in PBS, and cells were incubated at room temperature for 1 h. After three 5-min washes in PBS and 5 min of 1:5,000 DAPI staining, the cells were embedded with Mowiol. Analysis of clustering was performed as follows. Three independent transfections, each performed applying newly thawed and cultured C2C12 cells, were differentiated for 6 days with differentiation medium (DMEM, 5% horse serum, and 1% penicillin/streptomycin) and subjected to BTX staining. Myotubes showing BTX signals larger than 5 μm in length in a circumferential area of 10 μm around a transfected nucleus, as indicated by the green fluorescence of GFP-NLS, were counted in relation to the transfected tubes. Every tube was only counted once even if multiple nuclei were transfected to minimize confounding effects. This proportion for each condition was normalized to the respective proportion observed in pcDNA3-transfected controls from each transfection set, and the values were plotted and analyzed using GraphPad Prism.

Statistical Analysis—Data are presented as the mean values, and the error bars indicate ±S.D. The number of biological replicates per experimental variable (n) is usually >5 or as indicated in the figure legends. The significance was calculated by unpaired two-tailed t test or as indicated by the figure legends and is provided as real p values that are categorized for different significance levels: ***, $p < 0.001$; **, $p < 0.01$; or *, $p < 0.05$.

Results

Rapsyn, Dok-7, Rac1, and 14-3-3γ Interact with Protein Kinase CK2—Previously, we performed yeast two-hybrid screens and detected the interaction of protein kinase CK2 (subunit β and to a weaker extent subunit α) with the receptor tyrosine kinase MuSK at the NMJ (1). Here, we addressed whether other proteins that are located at the NMJ are also able to interact with CK2. To this end, we used GST fusion proteins of protein kinase CK2 subunit α or β with cell lysates of HEK293 cells that were transiently transfected with plasmids overexpressing one of the following genes for GST pulldown assays: AChRα, AChRβ, AChRγ, AChRδ, AChRε, MuSK, Rapsyn, Dok-7, Src, RhoA, Rac1, Cdc42, 14-3-3γ, Dsh, and the cytosolic domain of Lrp4 (Fig. 1*a*). As reported previously, MuSK and Dsh interacted with CK2β and to lower extent with CK2α (Fig. 1*a*) (1, 15). An almost similar interaction strength with both subunits of CK2 was detected for Rapsyn and Rac1 (Fig. 1*a*). 14-3-3γ and Dok-7 interacted better with CK2β than

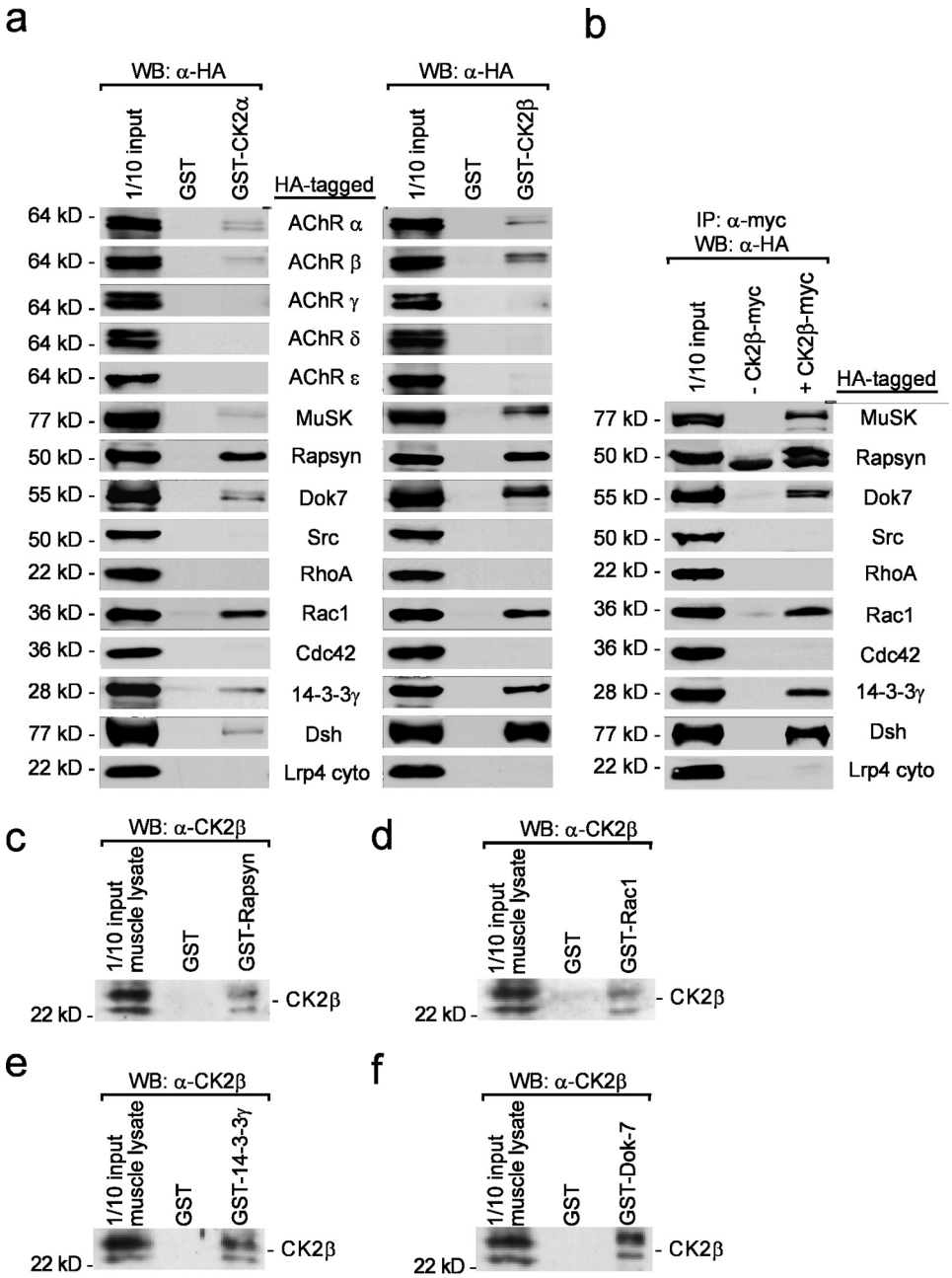

FIGURE 1. **Searching for proteins interacting with protein kinase CK2 at the mammalian NMJ.** *a*, proteins known to be localized at the NMJ were produced by HEK293 cells (HA-tagged) and used for GST pulldown assays together with purified recombinant GST-CK2α or GST-CK2β subunits of protein kinase CK2. Images of typical membranes after SDS-PAGE and Western blotting (*WB*) are presented. Note, for comparison, each time $^1/_{10}$ of the input is shown. *b*, apart from AChR subunits, all other potential CK2 interactors were confirmed by co-immunoprecipitation (*IP*) studies. To this end, all protein-expressing plasmids were transfected into HEK293 cells, and lysates used for precipitation of the indicated CK2 subunits (myc tag-labeled) and analyzed for co-precipitations of CK2 interactors (HA tag-labeled). Images show membranes after SDS-PAGE and Western blotting. Note, the lower of the two bands visible for Rapsyn belongs to the antibody chain, which is detected by the secondary antibody. *c–f*, GST pulldown verified interaction of Rapsyn, Rac1, 14-3-3γ, and Dok-7 with endogenous protein kinase CK2β from wild type mouse hind limb muscles. Images show membranes after SDS-PAGE and Western blotting. *cyto*, cytosolic domain.

CK2α (Fig. 1*a*). Two of the AChR subunits (α and β) appeared to weakly interact with both CK2 subunits (Fig. 1*a*). Next, co-immunoprecipitations were implemented to verify protein/protein interactions between CK2β and Rapsyn, Rac1, 14-3-3γ, and Dok-7 (Fig. 1*b*). In fact, all these proteins interacted again with CK2β as well as with the previously known interactors MuSK and Dsh (Fig. 1*b*). Furthermore, we confirmed these interactions in a more physiological context by using GST fusion proteins of Rapsyn, Rac1, 14-3-3γ, and Dok-7 to pull down endogenous CK2β from hind limb muscle cell lysates of wild type mice (Fig. 1, *c–f*).

Identification of the Interacting Epitope of Rapsyn with CK2: CK2 Does Not Phosphorylate Rapsyn in Vitro—To gain a better understanding of how CK2 interacts with Rapsyn, the epitope of Rapsyn that interacts with CK2β was mapped. Three mutants of Rapsyn were cloned, all of which carry differentially combined deletions of the RING domain, coiled coil motif, or only the amino-terminal domain until the end of TPR4 (Fig.

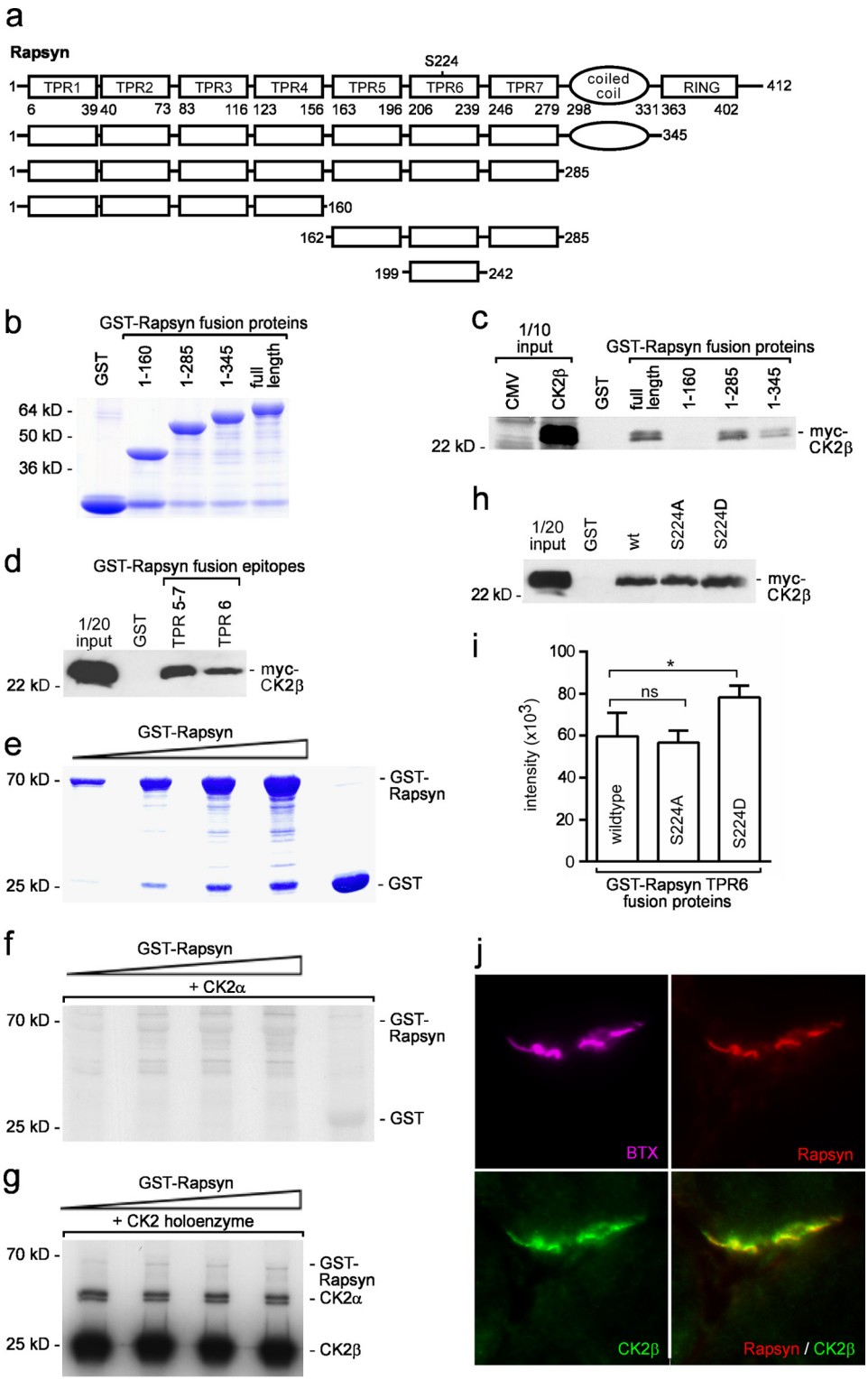

FIGURE 2. **Protein kinase CK2 interacts with Rapsyn but does not phosphorylate it.** *a*, scheme depicting topology of Rapsyn with its known epitopes. Mutant sizes are shown below the full-length Rapsyn protein. *b*, image showing Coomassie-stained SDS-PAGE of GST and GST-Rapsyn fusion proteins as indicated. *c*, GST-Rapsyn fusion proteins were used to pull down CK2β protein. The input control of HEK293 cell lysates of CK2β-expressing cells is shown as indicated. Note, Rapsyn amino acid residues 1–160 are not sufficient to bind to CK2. *d*, both internal domains of Rapsyn, TPRs 5–7 and TPR6, are able to pull down protein kinase CK2β. The image shows a Western blot membrane that is stained by anti-myc antibody. *e*, fusion proteins composed of GST and full-length Rapsyn were produced in bacteria, purified, and subjected to SDS-PAGE and Coomassie staining. The same amounts were used for *in vitro* phosphorylation assays as shown in *f* and *g*. *f* and *g*, [γ-^{32}P]ATP incorporation assays were performed with different amounts of GST-Rapsyn protein as shown in *e*. In *f*, only CK2α was used for kinase activity, whereas in *g*, CK2 holoenzyme was utilized. Note, CK2 holoenzyme phosphorylates CK2α and CK2β subunits but not Rapsyn. *h*, a phosphomimetic Rapsyn mutant pulls down more CK2β than wild type or alanine inactive Dok-7 mutants. The image shows a Western blot membrane after SDS-PAGE and staining. *i*, quantification of *h* as calculated from three independent GST pulldown assays. *j*, typical image of frozen hind limb cross-sections of wild type mice stained by CK2β and Rapsyn-specific antibodies. NMJs are labeled by Alexa Fluor 647-coupled BTX. The *error bars* indicate $\pm$S.D. *, $p < 0.05$; *ns*, not significant.

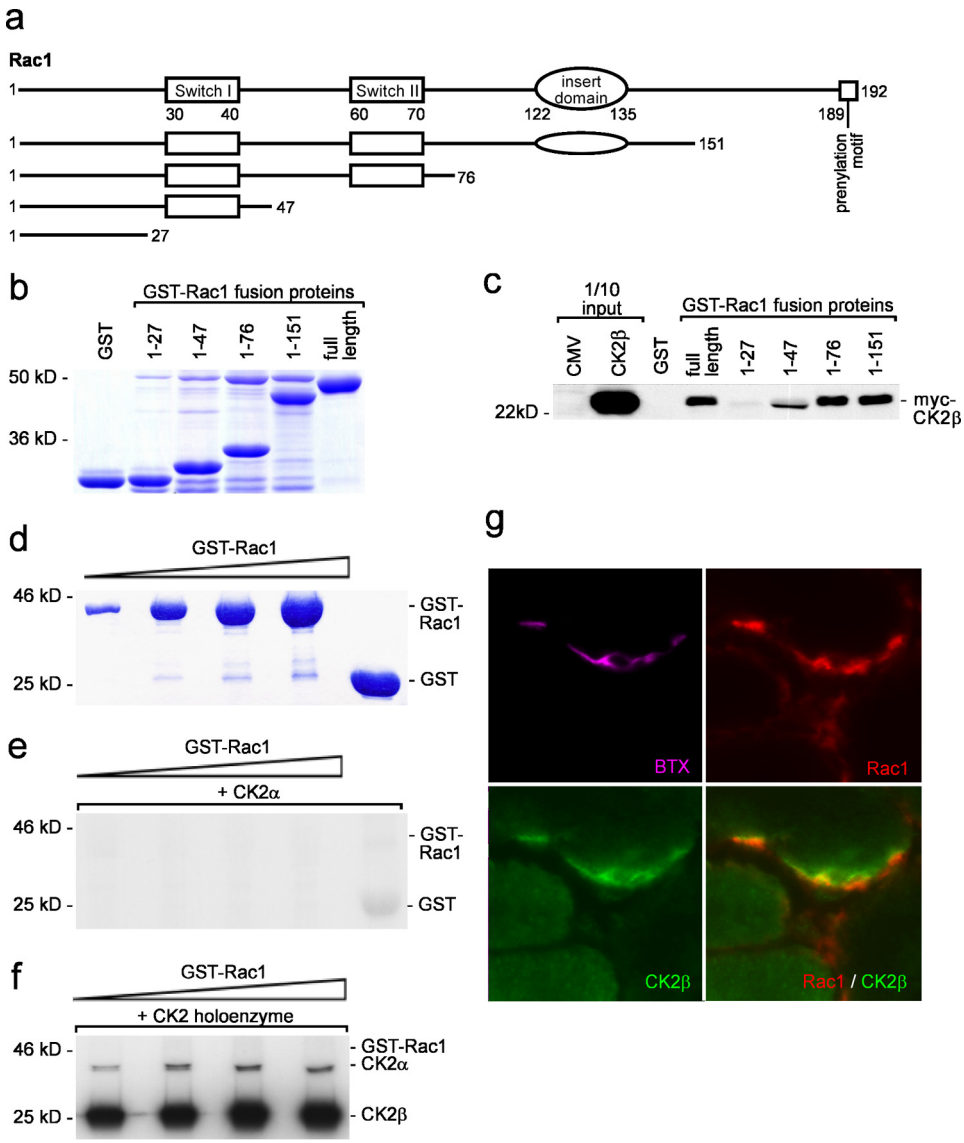

FIGURE 3. **Rac1 interacts with protein kinase CK2 by its Switch I domain.** *a*, schematic diagram showing the full-length Rac1 protein and its Switch regions, which change conformation on GDP/GTP exchange; its insert domain; and its prenylation motif at its carboxyl-terminal end. All Rac1 mutants truncated from their carboxyl-terminal end are shown underneath. *b*, image showing Coomassie-stained SDS-polyacrylamide gel of GST-Rac1 fusion proteins extracted from transfected HEK293 cells, purified, and separated by size. *c*, image showing a Western blot membrane of CK2β, which was pulled down by GST-Rac1 fusion proteins as indicated. Note, a Rac1 mutant that lacks the Switch I domain does not pull down CK2β. *d*, full-length Rac1 protein was fused to GST, expressed in bacteria, and purified for use in an *in vitro* phosphorylation assay. Increasing amounts of purified GST-Rac1 protein were verified by SDS-PAGE and Coomassie staining. *e* and *f*, the ability of CK2 to phosphorylate Rac1 was analyzed by [γ-^{32}P]ATP incorporation assays. Purified GST-Rac1 fusion protein was incubated with CK2α or CK2 holoenzyme, and phosphorylation events were detected by SDS-PAGE and autoradiography. *g*, typical image of frozen hind limb cross-sections of wild type mice stained by CK2β- and Rac1-specific antibodies. NMJs are labeled by Alexa Fluor 647-coupled BTX.

2*a*). The DNAs encoding these Rapsyn protein fragments were fused in-frame to GST, and recombinant fusion proteins were purified from bacteria and used for GST pulldown assays. The qualities of the purified GST-Rapsyn fusion proteins were confirmed by SDS-PAGE (Fig. 2*b*). Rapsyn variants were able to pull down CK2β as long as they contained TPRs 5–7 (Fig. 2*c*). To further narrow the epitope of Rapsyn that interacts with CK2β, we generated additional Rapsyn mutants composed only of TPRs 5–7 or TPR6, respectively. Both Rapsyn fragments were able to interact with CK2β (Fig. 2*d*). We conclude that TPR6 of Rapsyn is sufficient to mediate interaction with CK2β. We next asked whether protein kinase CK2 phosphorylates Rapsyn. Increasing amounts of purified recombinant GST-Rapsyn fusion protein were incubated together with recombinant CK2 and subjected to a [γ-^{32}P]ATP incorporation assay (Fig. 2, *e*–*g*). These experiments were done by applying catalytically active CK2α subunit or CK2 holoenzyme. In none of these experiments was CK2 able to phosphorylate the GST part of the fusion protein (Fig. 2*f*). Neither CK2α nor CK2 holoenzyme was able to phosphorylate any Rapsyn protein, not even by using high amounts of Rapsyn (Fig. 2, *f* and *g*). When CK2 holoenzyme was used, phosphorylation of both CK2α and CK2β subunits by CK2 itself was detected (Fig. 2*g*). Interestingly, we identified *in silico* (KinasePhos 2.0) serine 224 of Rapsyn within a strongly suitable phosphorylation motif for CK2 (Fig. 2*a*). Although we did not detect any Rapsyn phosphorylation by CK2 *in vitro*, we cannot rule

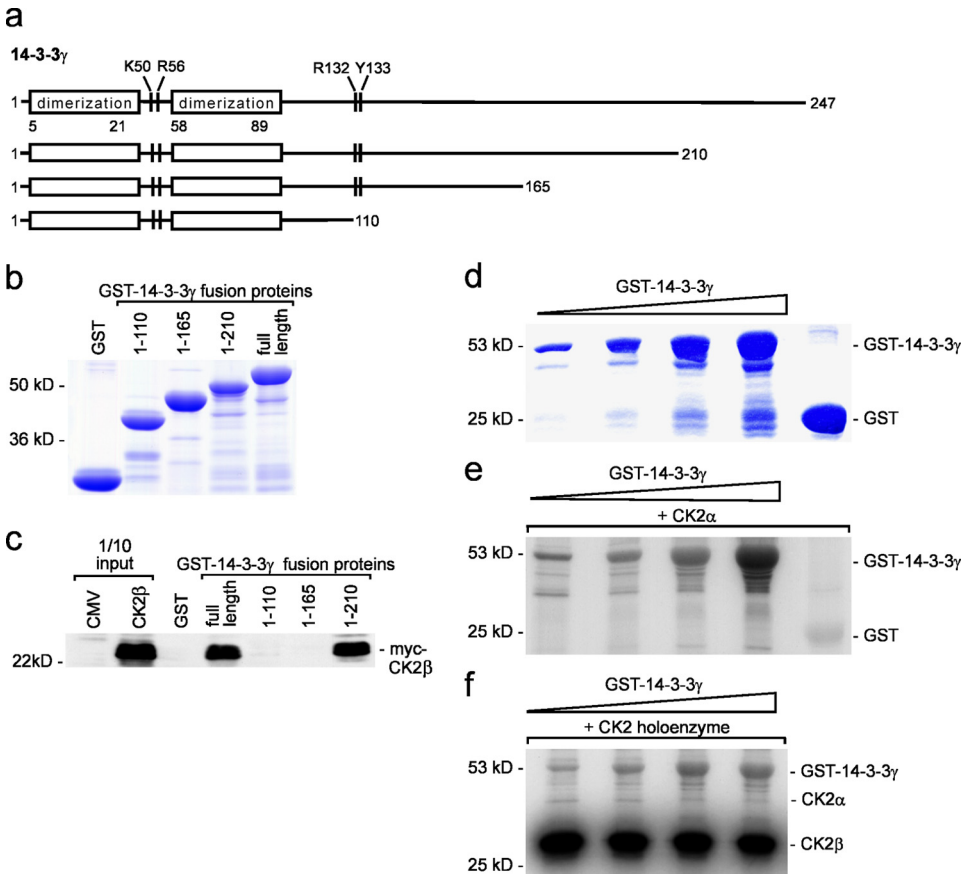

FIGURE 4. **Protein kinase CK2 interacts and phosphorylates 14-3-3γ.** *a*, topography of full-length 14-3-3γ and its carboxyl-terminally truncated variants. *b*, full-length 14-3-3γ and its carboxyl-terminally truncated mutants were purified as GST fusion proteins, and their quality was verified by SDS-PAGE and Coomassie staining. *c*, GST-14-3-3γ fusion proteins were utilized to pull down CKβ. Precipitates were analyzed by SDS-PAGE, and the image of a typical Western blot membrane is shown. *d*, recombinant GST-14-3-3γ protein was purified from bacterial lysates, and its quality was verified by SDS-PAGE and Coomassie staining. *e* and *f*, *in vitro* phosphorylation assays were performed to determine whether CK2 is able to phosphorylate 14-3-3γ. CK2 was used either as the holoenzyme (*f*) or as its catalytically active α subunit (*e*). Images were taken from autoradiographs. Note, 14-3-3γ is significantly phosphorylated by CK2.

out the possibility that CK2 phosphorylates Rapsyn *in vivo*. To this end, we investigated binding patterns of Rapsyn mutants with CK2β. In fact, a phosphomimetic Rapsyn mutant (Ser-224 to Asp) was able to pull down more CK2β than wild type Rapsyn protein (Fig. 2, *h* and *i*). By immunofluorescence studies, we confirmed co-localization of Rapsyn and CK2β at NMJs of hind limb gastrocnemius/soleus muscle of wild type mice (Fig. 2*j*). Altogether, protein kinase CK2 interacts with TPR6 epitope of Rapsyn but does not phosphorylate it *in vitro*.

Identification of the Epitope of Rac1 That Interacts with CK2—Next, the nature of the interaction between Rac1 and CK2 was characterized. Four Rac1 mutants were generated by different truncations of wild type Rac1 at its carboxyl-terminal end (Fig. 3*a*). The full-size Rac1 and its mutants were fused to GST, recombinantly expressed, and purified from bacteria. The qualities of the purified proteins were confirmed by SDS-PAGE (Fig. 3*b*). Loss of the Switch I domain of Rac1 abolished its interaction with CK2β (Fig. 3*c*). Subsequently, we asked whether CK2 phosphorylates Rac1. To this end, increasing amounts of recombinant GST-Rac1 protein were incubated together with CK2α or the whole CK2 holoenzyme. The grade of purity of GST-Rac1 was verified by analyzing increasing protein amounts by SDS-PAGE (Fig. 3*d*). Using *in vitro* phosphorylation assays, we failed to detect CK2 phosphorylation of any Rac1 (Fig. 3, *e* and *f*). Only CK2 subunits α and β were phosphorylated by CK2 itself (Fig. 3*f*). Finally, a perfect co-localization was detected between CK2β and Rac1 on frozen sections of wild type murine hind limb muscle by immunofluorescence staining (Fig. 3*g*).

Protein kinase CK2 Interacts with the Carboxyl-terminal Domain of 14-3-3γ and Phosphorylates It—A number of carboxyl-terminal truncations of 14-3-3γ protein were generated, purified as recombinant proteins, quality-controlled by SDS-PAGE, and subjected to GST pulldown assays (Fig. 4, *a–c*). The carboxyl-terminal part of the 14-3-3γ protein, ranging from amino acid residues 166 to 210, was required for interaction with CK2β (Fig. 4*c*). *In vitro* phosphorylation experiments with increasing amounts of purified GST-14-3-3γ protein, radioactive [γ-^{32}P]ATP, and CK2 revealed that CK2 phosphorylates 14-3-3γ in a dose-dependent fashion (Fig. 4, *d–f*). Moreover, 14-3-3γ and CK2β were co-localizing on frozen murine hind limb sections of wild type mice visualized by immunofluorescence staining (Fig. 5*e*).

Protein Kinase CK2 Phosphorylates 14-3-3γ at Serine Residue 235—To identify serine and threonine residues of 14-3-3γ that are phosphorylated by CK2, 14-3-3γ was dissected into four different parts (Fig. 5*a*). Each protein fragment of 14-3-3γ was purified as a GST fusion protein and *in vitro* phosphorylated by CK2 (Fig. 5, *b* and *c*). A deletion mutant of 14-3-3γ consisting of

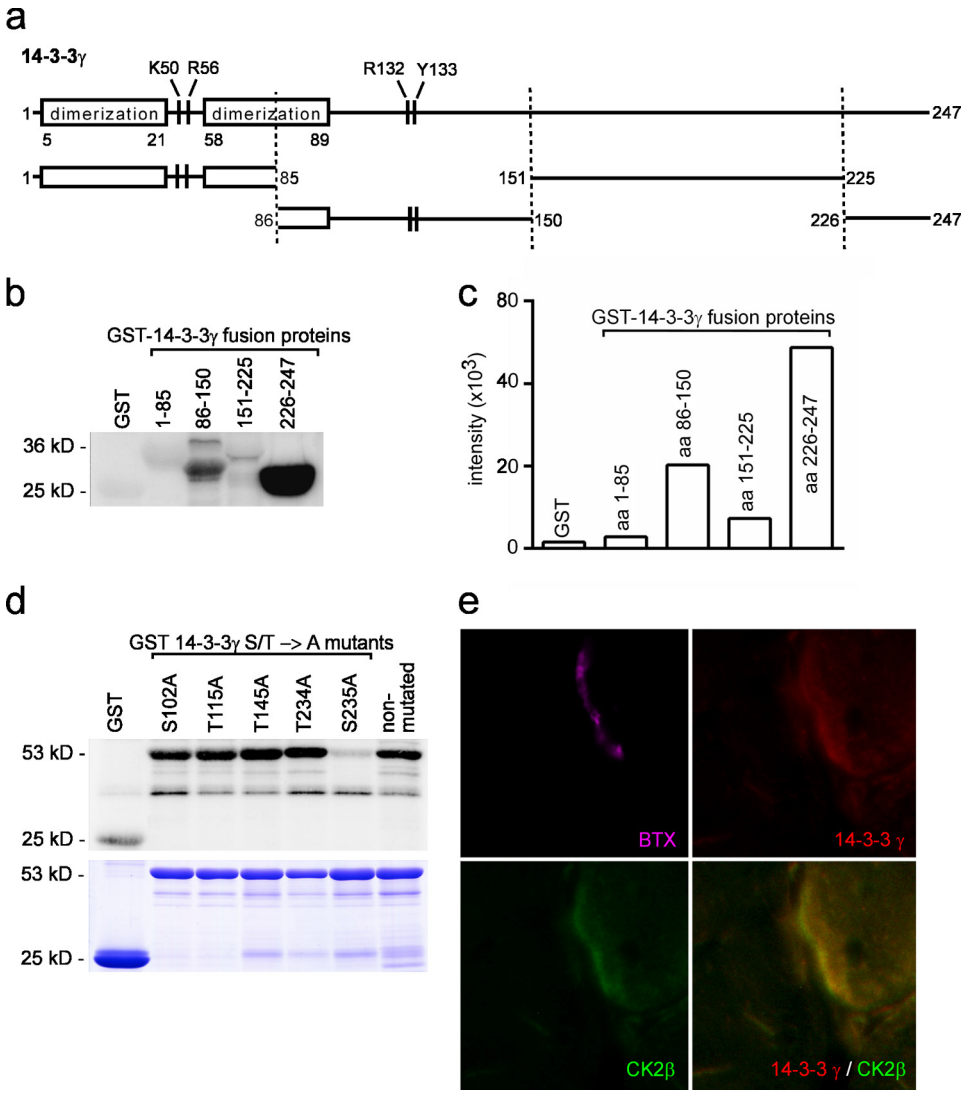

FIGURE 5. **Protein kinase CK2 phosphorylates 14-3-3γ at serine residue 235.** *a*, to identify potential CK2 target sites, 14-3-3γ was divided into four fragments. Full-length 14-3-3γ and its fragments are depicted. *b* and *c*, each of the 14-3-3γ fragments as shown in *a* were fused to GST, purified from bacteria, and used for *in vitro* phosphorylation assays with CK2. Reaction mixtures were separated by SDS-PAGE, and phosphorylated 14-3-3γ proteins were detected by autoradiography (*b*). Note, only GST-14-3-3γ aa86–150 and aa226–247 (much more strongly) were phosphorylated by CK2. Quantified band intensities are presented as a graph (c). *d*, to identify potential CK2 target sites within the GST-14-3-3γ aa86–150 and aa226–247 fragments, software algorithms were used (KinasePhos 2.0). Potential amino acid residues were substituted by alanine, and respective full-length 14-3-3γ mutants were analyzed for *in vitro* phosphorylation by CK2. Reaction mixtures were subjected to SDS-PAGE, and bands were detected by autoradiography. Note, substitution of serine 235 of 14-3-3γ to alanine completely abolished CK2-dependent phosphorylation. *e*, typical image of frozen hind limb cross-sections of wild type mice stained by CK2β- and 14-3-3γ-specific antibodies. NMJs are labeled by Alexa Fluor 647-coupled BTX.

amino acid residues 226–247 was very prominently phosphorylated as quantified by densitometric analysis of the autoradiograph (Fig. 5*c*). All potential CK2 target sites within the fragment of 14-3-3γ ranging from amino acid residues 226 to 247 were identified by KinasePhos 2.0 algorithm or predicted by amino acid sequence (Table 1).[4] Serine residues at potential CK2 target sites of 14-3-3γ were substituted by alanine residues. Only the 14-3-3γ mutant carrying an alanine substitution at serine 235 was not phosphorylated by CK2 (Fig. 5*d*).

Protein Kinase CK2 Interacts with and Phosphorylates Dok-7—First, several deletion mutants of Dok-7 were generated to extract purified recombinant mutant Dok-7 proteins (Fig. 6, *a* and *b*). All Dok-7 mutant proteins were able to interact with CK2β as long as they contained the PH domain of Dok-7 (Fig. 6, *c* and *d*). In particular, a mutant Dok-7 protein lacking its amino-terminal end up to residue 108 (this part of the Dok-7 consists of the PH domain) failed to interact with protein kinase CK2 (Fig. 6*d*). Second, increasing amounts of GST-Dok-7 were incubated together with CK2α or CK2 holoenzyme and radioactive [γ-^{32}P]ATP to determine whether CK2 phosphorylates Dok-7 (Fig. 6, *e*–*g*). CK2-dependent phosphorylation of Dok-7 was easily detectable (Fig. 6, *f* and *g*). Finally, we identified Dok-7 co-localization with CK2β at the NMJs of frozen hind limb sections by immunofluorescence staining (Fig. 7*d*).

Protein Kinase CK2 Intensively Phosphorylates Dok-7—To identify which serine or threonine residues of Dok-7 are phosphorylated by CK2, the full-length Dok-7 protein was divided

[4] L. A. Pinna, personal communication.

TABLE 1

Potential CK2-dependent phosphorylation sites of 14-3-3γ and Dok-7 as predicted by KinasePhos 2.0

Prediction scores are given next to the amino acid residues. Band intensities, as extracted from *in vitro* phosphorylation assays using Image J, are presented for each analysed amino acid residue of 14-3-3γ and Dok-7 phosphorylated by CK2. In some cases, several amino acid residues were mutated on the same protein fragment as indicated by the boxes within the table. np, not predicted.

14-3-3γ	Score	Intensity
S38	0.795	
S64	0.702	
S71	0.540	
S102	0.582	0,945
T115	np	1,008
T145	0.587	1,184
T210	0.644	
S215	0.659	
T234	0.551	1,075
S235	np	0,123

Dok-7	Score	Intensity
T122	0.509	
T130	0.621	
T147	0.507	
S185	0.859	
T206	0.739	
S225	0.974	
S249	np	0,416
S251	np	0,864
S256	0.944	1,025
S262	np	0,751
S264	np	
S265	0.600	1,072
S266	0.945	0,948
S267	np	
S268	np	
S271	np	0,849
S273	np	0,470
S276	np	0,967
S278	np	
S279	np	
S282	np	1,079
S288	np	
S289	np	
S290	np	
S291	np	
T294	0.838	0,936
S295	np	
S315	np	1,071
S334	0.925	0,833
S335	np	
S336	np	
S338	np	0,546
T342	0.500	0,928
S344	np	0,870
S346	np	
S347	np	
S351	0.500	
S358	0.722	
S380	0.910	
S431	0.945	
S470	0,749	

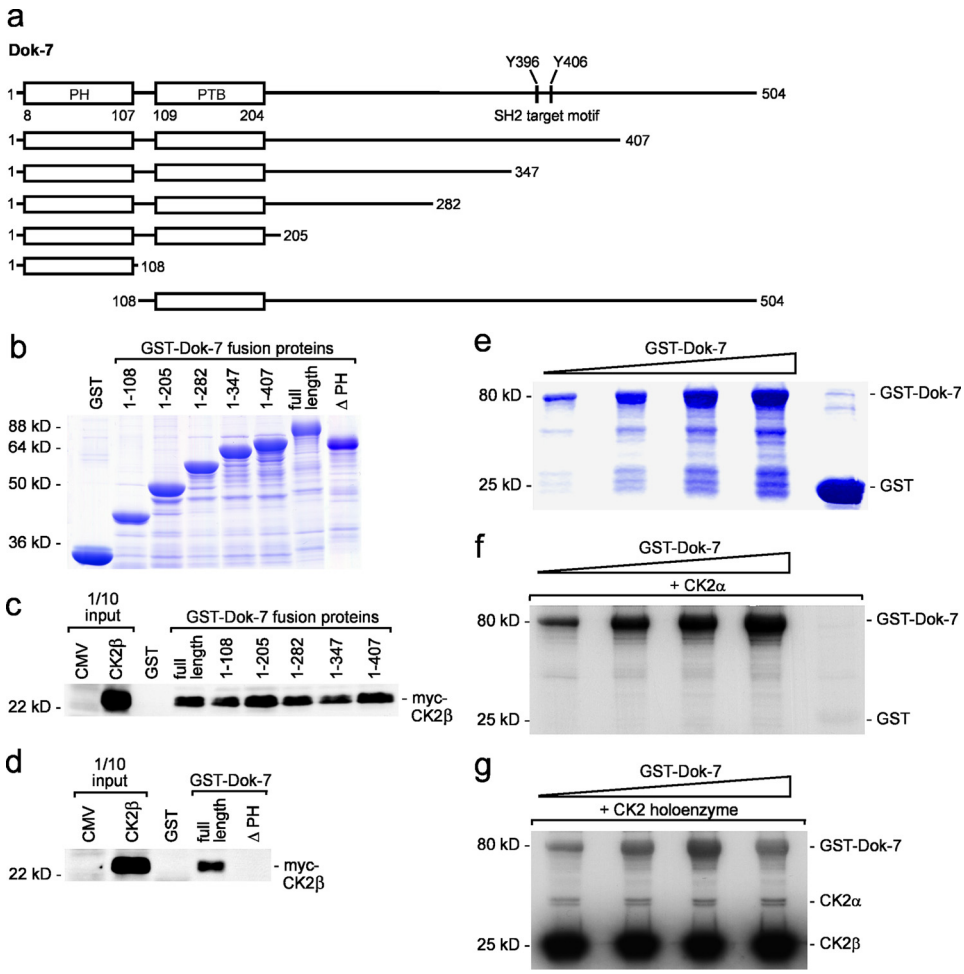

FIGURE 6. **Signaling adaptor protein Dok-7 binds by its pleckstrin homology domain to protein kinase CK2.** *a*, Dok-7 protein presented schematically. Several deletion mutants of Dok-7 are depicted underneath. *PTB*, phosphotyrosine binding domain; *SH2*, Src homology 2 domain. *b*, full-length and different Dok-7 deletion mutants were purified (recombinant GST fusion proteins), and their quality was inspected by SDS-PAGE and Coomassie staining. *c* and *d*, GST-Dok-7 fusion proteins were used to pull down CK2β. Reaction mixtures were monitored by SDS-PAGE and Western blotting. Note, the pleckstrin homology domain is necessary and sufficient for interaction with protein kinase CK2. *e*, full-length Dok-7 protein was fused to GST, purified, and quality-controlled by loading increasing amounts for SDS-PAGE, and analyzed by Coomassie staining. Note, the same amounts of protein were used for *in vitro* phosphorylation experiments as shown in *f* and *g*. *f* and *g*, [γ-^{32}P]ATP incorporation assays were performed by incubating CK2α or CK2 holoenzyme with full-length Dok-7 protein and radiolabeled [γ-^{32}P]ATP. After SDS-PAGE size separation, bands were detected by autoradiography. Note, CK2 is able to phosphorylate Dok-7.

into six different protein fragments (Fig. 7*a*). Each of these Dok-7-encoding DNA fragments were fused in-frame to GST, expressed, purified as recombinant protein, and phosphorylated by CK2 *in vitro*. Intriguingly, except for Dok-7 amino-terminal amino acid residues 38–157 encompassing the interaction site with CK2 and part of the phosphotyrosine binding domain, all other Dok-7 fragments were phosphorylated by CK2 (Fig. 7*b*). Quantitative scans of the autoradiographs revealed that Dok-7 fragments comprising amino acid residues 238–282 and 283–347 were intensively phosphorylated by CK2 (Fig. 7*c*). The primary structure of Dok-7 was analyzed by KinasePhos 2.0 algorithm for CK2 target sites (Table 1), and numerous potential amino acid residues were identified (Table 1).

Protein Kinase CK2 Phosphorylates Dok-7 at Many Different Serine Residues—CK2 seems to phosphorylate many amino acid residues of Dok-7 protein (Fig. 7*b*). We decided to identify only potential phosphorylation sites within the two Dok-7 fragments ranging from amino acid residues 238 to 347 as obviously these fragments featuring amino acid residue 238–282 and 283–347, respectively, were the most strongly phosphorylated (Figs. 7*c* and 8*a*). To address this issue, several potential CK2 target sites within GST-Dok-7 fragment aa238–282 were substituted by alanine residues. These purified mutant recombinant proteins were subjected to *in vitro* phosphorylation assays together with CK2 (Fig. 8, *b*–*d*). All band intensities of phosphorylated GST-Dok-7 fragment aa238–282 alanine mutants were quantified (see also Table 1). It appeared likely that serines 249, 266, and 273 were all involved in CK2-dependent phosphorylation of the GST-Dok-7 fragment aa238–282 (Fig. 8, *b*–*d*, and Table 1). We also analyzed potential CK2-dependent phosphorylation sites of the GST-Dok-7 fragment aa283–347 (Fig. 8*a*). A number of serine and threonine residues of the GST-Dok-7 fragment aa283–347 were substituted by alanines (Table 1). After purifying these recombinant mutant GST-Dok-7 fragments, they were used for *in vitro* phosphorylation assays with CK2 (Fig. 8, *e*–*g*), and the autoradiographs were scanned, normalized, and quantified (Table 1). After normal-

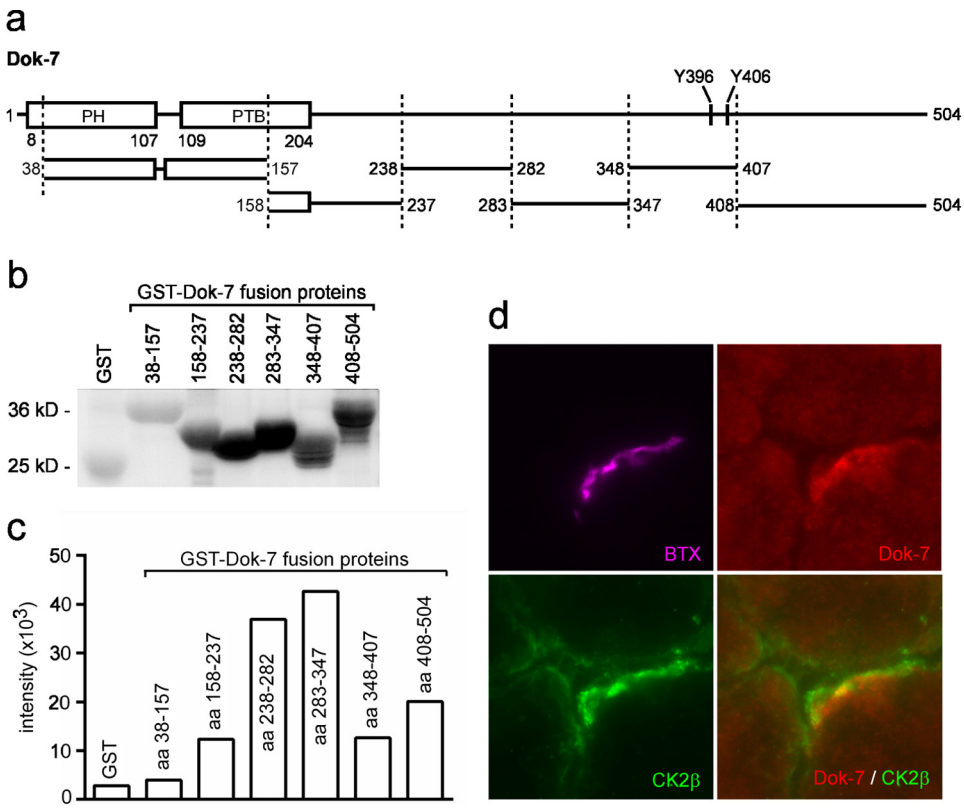

FIGURE 7. **Dok-7 is intensively phosphorylated by protein kinase CK2.** *a*, to identify CK2 target sites within the primary structure of Dok-7, the protein Dok-7 was divided into six fragments. Full-length Dok-7 and the generated fragments are depicted. *PTB*, phosphotyrosine binding domain. *b* and *c*, all six Dok-7 fragments were utilized for *in vitro* phosphorylation assays and analyzed by SDS-PAGE and autoradiography (*b*). Band intensities were quantified to reflect phosphorylation degree (*c*). Note, almost all Dok-7 fragments were phosphorylated by CK2, and Dok-7 fragments aa238–282 and aa283–347 exhibited the highest amounts of radioactivity (*c*). *d*, typical image of frozen hind limb cross-sections of wild type mice stained by CK2β- and Dok-7-specific antibodies. NMJs are labeled by Alexa Fluor 647-coupled BTX.

ization, substitutions showed that a number of serine residues appear to be involved in CK2-dependent phosphorylation of the GST-Dok-7 fragment aa283–347, namely serine residues 289, 290, 291, 335, 336, 338, 346, and 347 (Fig. 8, *e–g*, and Table 1). Lack of phosphorylation was obvious by autoradiography of a Dok-7 mutant where serine residues 346 and 347 were substituted by alanines, but other substitutions also led to diminished phosphorylation that was recognized after normalization (Fig. 8*f* and Table 1). Interestingly, Dok-7 proteins from different species have a highly conserved stretch of amino acid residues encompassing 327–355 (see Fig. 10).

Phosphorylation of Dok-7 by CK2 Influences the AChR Aggregation Ability of Dok-7 in Myotubes—Overexpression of Dok-7 is known to be sufficient for aggregation of AChRs in myotubes (13). We wondered whether CK2-dependent Dok-7 phosphorylation might influence Dok-7 function regarding aggregation of AChRs. To this end, we generated inactive alanine and phosphomimetic aspartate and glutamate Dok-7 mutants where we replaced several of the serine residues phosphorylated by CK2 (serine residues 249, 264, 265, 266, 273, 346, and 347). The expression of all Dok-7 mutants was confirmed by transfection into HEK293 cells and Western blotting (Fig. 9*a*). After transfection of the Dok-7 mutant-expressing plasmids into C2C12 myoblasts and differentiation to myotubes, we monitored AChR aggregation by BTX staining (Fig. 9*b*). Indeed, phosphomimetic Dok-7 mutants aggregated AChRs with significantly higher frequency than wild type or inactive alanine mutants (Fig. 9*b*). However, the morphology of Dok-7-induced AChR aggregation was not obviously altered (Fig. 9*c*).

Discussion

Here, we show for the first time that protein kinase CK2 strongly interacts with proteins Rapsyn, Rac1, 14-3-3γ, and Dok-7, which are all implicated in the postsynaptic apparatus of the NMJ (Fig. 1). A weak interaction with several AChR subunits was also detected but is beyond the scope of this study (Fig. 1*a*). Another interaction partner of protein kinase CK2 is Dsh (Fig. 1, *a* and *b*). Previously, protein kinase CK2 was reported to associate with and phosphorylate the central domain of Dsh (15). Moreover, Dsh was shown to regulate clustering of AChRs by interacting with MuSK (16). In accordance with those data, we performed a KinasePhos screen to predict CK2-dependent phosphorylated serine and threonine residues within the primary structure of Dsh. With >90% specificity, serine residues 202, 213, and 344 are likely phosphorylated by protein kinase CK2, with serine 213 having an >99% specificity. These serine residues are positioned within the central domain of Dsh and are in agreement with previously published data, which implicate this domain to be phosphorylated (15). Overexpression of Dfz2, a wingless receptor, was shown to stimulate

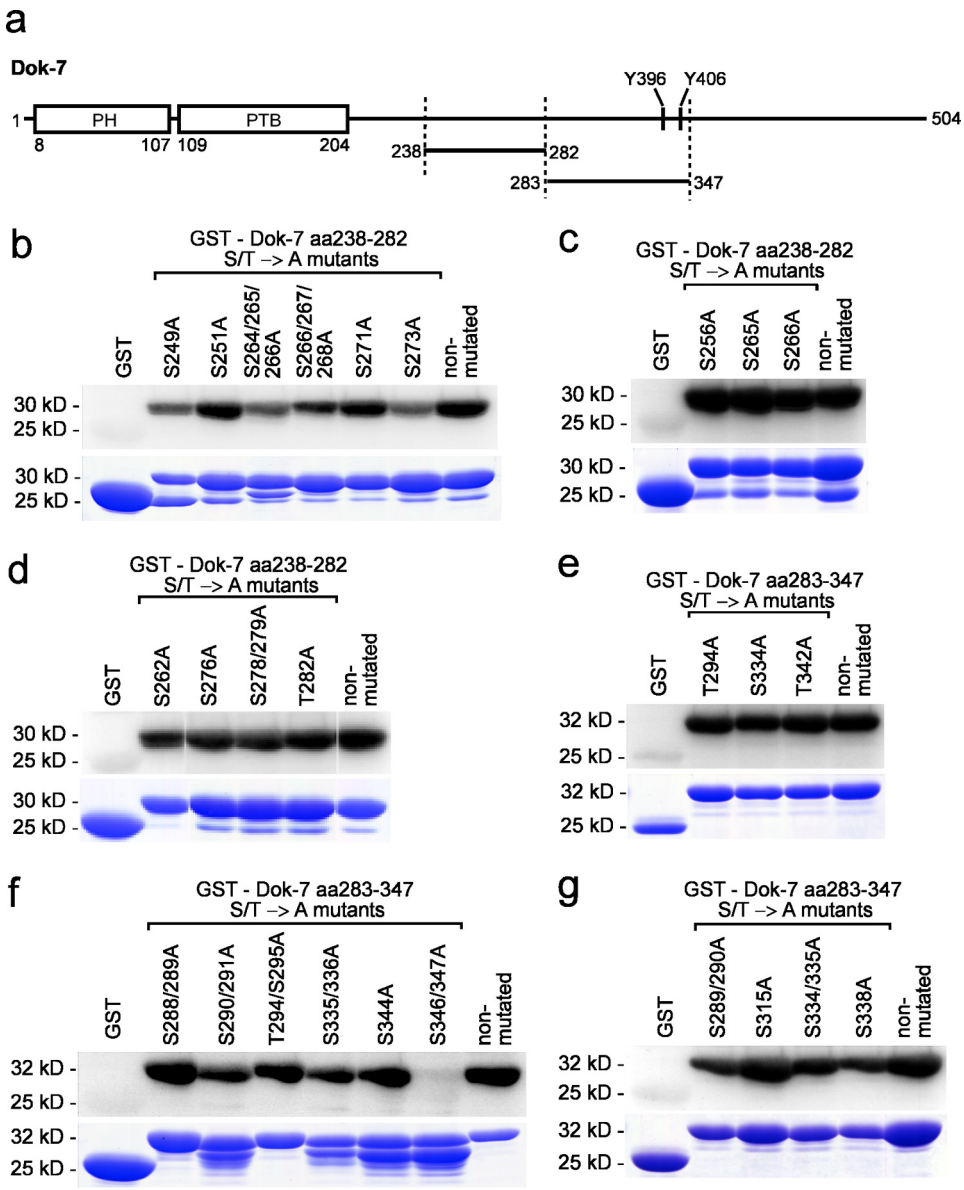

FIGURE 8. **A systematic approach to identify amino acid residues of Dok-7 phosphorylated by CK2.** *a*, scheme depicting the location of Dok-7 fragments aa238–282 and aa283–347 in comparison with the topology of full-length Dok-7. *PTB*, phosphotyrosine binding domain. *b–d*, potential CK2 target sites within Dok-7 fragment aa238–282 were predicted by KinasePhos 2.0, substituted by alanine residues, and analyzed by *in vitro* phosphorylation assays. Reaction mixtures were subjected to SDS-PAGE for size separation, and bands were detected by autoradiographs. Band intensities were quantified by ImageJ and are presented in Table 1. Note, several Dok-7 mutants contain more than one alanine substitution. *e–g*, similar to *b–d* but with the exception that all experiments were done with the Dok-7 fragment aa283–347.

phosphorylation of Dsh by CK2, suggesting a role for CK2 in Wnt signal cascades (15).

All protein kinase CK2 binding partners at the NMJ that are known up to now, are summarized in Table 2. Four of these were discovered by the present study.

Moreover, we provide evidence for CK2-dependent phosphorylation of 14-3-3γ and Dok-7, and we even identified several of these phosphorylated serine residues for both proteins. Our assays failed to detect any CK2-dependent phosphorylation of Rapsyn and Rac1. However, our data do not exclude a potential phosphorylation of Rapsyn and Rac1 at the NMJ as *in vivo* phosphorylation of Rapsyn or Rac1 might not be detectable by an *in vitro* approach. In fact, KinasePhos screens did not detect any potential CK2-dependent phosphorylation site for Rac1, but two hits were revealed for Rapsyn (Ser-224, prediction score of 0.814; Ser-369, prediction score of 0.564). Moreover, potential phosphorylation of serine residues of Rapsyn was indicated by experiments with *Torpedo* electrocytes (17). Here, we showed that a phosphomimetic Rapsyn mutant fused to GST was able to pull down more CK2β protein (Fig. 2*h*). Conversely, for Rac1, it was reported that phosphorylation of serine residue 71 modulates downstream signaling in cultured cells (18). Whether phosphorylation of Rapsyn and Rac1 serine or threonine residues occurs at neuromuscular synapses *in vivo* has to be approached by future experiments.

Recently, protein kinase CK2 was identified as a MuSK-interacting protein (1). CK2 was shown to stabilize postsynaptic AChR aggregates by MuSK phosphorylation (1). In light of

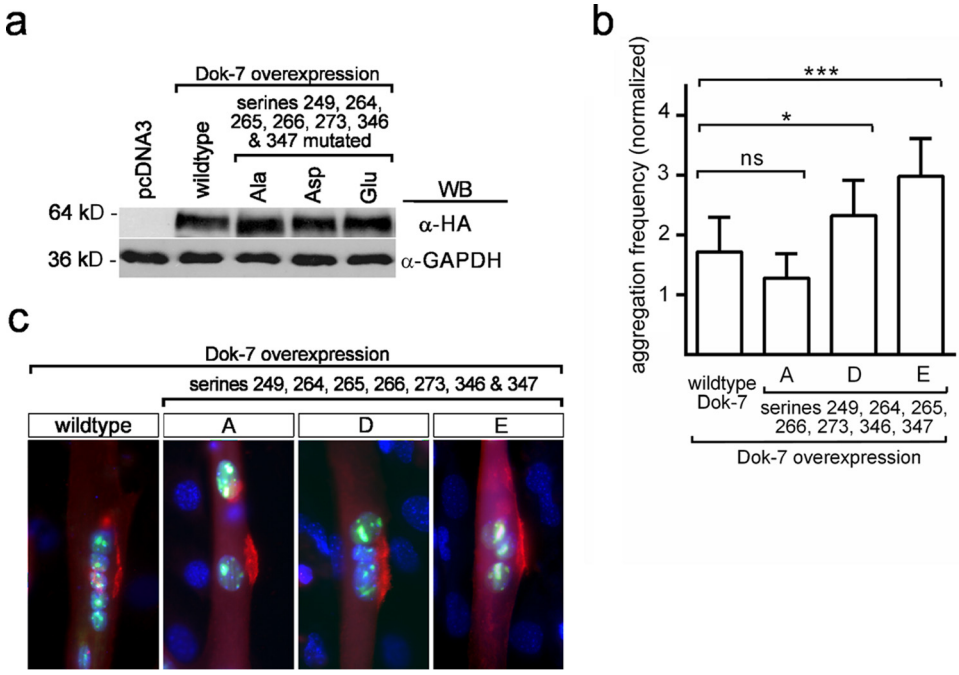

FIGURE 9. **Dok-7 inactive and phosphomimetic mutants perform differently in aggregation of AChRs.** *a*, all Dok-7 proteins were transfected in HEK293 cells, and their expression confirmed by SDS-PAGE and Western blotting (*WB*) in comparison with the housekeeping protein GAPDH. *b*, C2C12 cells were transfected with either of the different Dok-7 expression plasmids and GFP-NLS, differentiated to myotubes, and stained by rhodamine-coupled BTX and DAPI. Note, the graph indicates that GFP-NLS-positive myotubes aggregate AChRs much more frequently after introduction of Dok-7 phosphomimetic than with wild type or inactive Dok-7 protein. *c*, immunofluorescence staining of C2C12 myotubes. No obvious morphological change is detectable regardless of whether Dok-7 wild type or one of the mutants was transfected into the cells. The *error bars* indicate ±S.D. ***, $p < 0.001$; *, $p < 0.05$; *ns*, not significant.

TABLE 2

Summary illustrating the function of individual CK2 binding partners at the NMJ

Note that this is the first report about interaction of CK2β with Rapsyn, Rac1, 14-3-3γ, and Dok-7. In the case of these four proteins, the citations refer to the first descriptions of these proteins at the NMJ. n.a., not applicable.

CK2 interactors	Binding epitope	Phosphorylation	Function of binding CK2	Citation
Dishevelled	Central domain	n.a.	Unknown	15
MuSK	Kinase insert	Serines 680 and 697	Maintenance of NMJ	1
Rapsyn	TPR6	Ser-224 (?)	Unknown	30
Rac1	Switch I domain	n.a.	Unknown	
14-3-3γ	aa110–165	Ser-235	Unknown	12
Dok-7	PH domain	Serines 249, 266, 273, 289, 290, 291, 335, 336, 338, 346, 347	Improve AChR aggregation	13

those data, it is very intriguing that CK2 appears not only to interact with other NMJ members but also phosphorylates them. For 14-3-3γ, only serine residue 235 was phosphorylated by CK2 *in vitro* (Fig. 5*d*). A comparison of the primary structure of 14-3-3γ among different species (human, mouse, chick, frog, and zebrafish) revealed that they all have this serine 235 residue conserved (data not shown). Likewise, several serine residues of Dok-7 that were here identified to be phosphorylated by CK2 are mostly conserved within other species (Fig. 10). Evolutionary conservation of phosphorylatable amino acid residues of proteins between different species might reflect their biological importance (19).

It cannot be too strongly emphasized that this is the first description for potentially relevant serine phosphorylation of Dok-7 at the NMJ. Recently, an international phosphoproteomic effort provided evidence for phosphorylation of human Dok-7 serine residues in a different matter that might be indicative as a first hint for CK2-dependent Dok-7 phosphorylation at the NMJ (20).

To understand the biological role of the identified CK2-dependent phosphorylation events for both 14-3-3γ and Dok-7, generation of inactive or phosphomimetic mutants of these proteins will be necessary. These mutants might be used to study their impact in cultured muscle cells on AChR clustering or morphology. As a start, in the present study, phosphomimetic mutants of Dok-7 mimicking the posttranslational phosphorylation by CK2 were generated and shown to aggregate AChRs more frequently than wild type Dok-7 in C2C12 myotubes (Fig. 9*b*). Of course, the concomitant expression of the endogenous 14-3-3γ or Dok-7 proteins might influence the outcome of such experiments, but selective knockdown of both endogenous proteins by targeting UTRs of the respective mRNAs might be helpful to reduce their protein amounts in future studies. By this strategy, the biological effect of CK2-dependent phosphorylation of 14-3-3γ and Dok-7 proteins might be elucidated.

Besides interaction and phosphorylation, the epitopes of each of the four proteins found here to interact with CK2 were mapped. The binding of CK2 to Rapsyn was abolished after Rapsyn was truncated by its TPRs 5–7 (Fig. 2*c*). This might be of interest because the predicted phosphorylated serine residue 224 of Rapsyn (see above) is located within TPR6. In fact, fur-

```
Mus musculus       181 VFFLSSAEGEQMSFLFDCIVRGISPTKGPFGLRPVLPDPSSGGPSASEERVAQEALEALQ 240
Homo sapiens       181 VFFLSSAEGEQISFLFDCIVRGISPTKGPFGLRPVLPDPSPPGPSTVEERVAQEALETLQ 240
Xenopus tropicalis 181 VFFLSCADGDQISFLFDCIVRGISPTKGPFGLRPVLPDPNFN-PAYMEERVAH---ETLQ 236
Danio rerio        181 VFFLACADGEQISFLVDCIVRGISPSRGPFGLRPVLPDPNAN-PSSIEDRISQ---EASE 236
Nestor notabilis   144 VFFLSCAEGEQISFLFDCIVRGISPTKGPFGLRPVLPDPSPN-PAYSEERLAH---EALQ 199
                       ****:.*:*:*:***.*********::************.   *:  *:*:::   *: :

Mus musculus           LEKRLSLLSHSG----------RP-GSGGDDRSLSSSSSEASHSDISASSRLTAWPEQSS 289
Homo sapiens           LEKRLSLLSHAG----------RP-GSGGDDRSLSSSSSEASHLDVSASSRLTAWPEQSS 289
Xenopus tropicalis     LEKRLSLLSHHS----------LGDFISGDDRSLSSSSSDTSHSDASAGSRLTIWPEASS 286
Danio rerio            LEKRLSMLSICSHHSSAASTFSYGASLAGDDRSISSSSSEASHSDNSLGSRLAIWPEPVR 296
Nestor notabilis       LEKRLSLLSHTS----------RQ-GSGGDERSLSSSSSDTSHSDVSVGSRLTIWPEQSS 248
                       ******:**  .              .**:**:*****::** * * .***: ***

Mus musculus           SS-AGTS--------QEGPGL------VAAQG--------PGEAMLGASRPPLKPLRPRQ 326
Homo sapiens           SS-ASTS--------QEGPRP------AAAQA--------AGEAMVGASRPPPKPLRPRQ 326
Xenopus tropicalis     ASSASTS--------AESHGM------AAAKGIHLREERAYAE-AHRTSKPPPKPVQSRQ 331
Danio rerio            HPTPVEPPPPPPSSSSSSHLLVTGCKSTACSVSTSSDERIY-GVMMGGLRPPSKPPHPRG 355
Nestor notabilis       A---STS--------QESHGL------AAAKGIHLGEEKTLPEGAHGTTKPPPKPLRSRQ 291
                                      ..         .*..                 :** ** : *

Mus musculus           LQEVGRQSSSDSGIATGSHSSYSGSFSSYAGSNLDVWRAGEEFGSLLSLPPGAS------ 380
Homo sapiens           LQEVGRQSSSDSGIATGSHSSYSSSLSSYAGSSLDVWRATDELGSLLSLPA-AG------ 379
Xenopus tropicalis     LQEIGRQSSSDSGIATGSHSSYSGSFSSYAESL-DI-CHGEEFGSVLSLPLNLT------ 383
Danio rerio            LQEAGRQSSTDSGIATGSHSSYSGSFSSYTGSMDIGHGETDEFGSLISLPQNPNSVSIIN 415
Nestor notabilis       LQEIGRQSSSDSGIATGSHSSYSGSFSSYAGSL-DI-CHGDEFGSLLSLPLNFP------ 343
                       *** *****:*************.*:***: *        :*:**::***
```

FIGURE 10. **Alignment of Dok-7 from different species.** An *asterisk* indicates positions that have a single, fully conserved residue. A *colon* indicates conservation between groups of strongly similar properties, scoring >0.5 in the Gonnet PAM 250 matrix. A *period* indicates conservation between groups of weakly similar properties, scoring ≤0.5 in the Gonnet PAM 250 matrix. The alignment was made using the UniProt sequence alignment tool. Note, serine residues shown in *red* are likely to be phosphorylated by CK2.

ther experiments confirmed that TPR6 of Rapsyn is sufficient for interaction with CK2β (Fig. 2*d*). For Rapsyn self-clustering, only TPR1 and TPR2 are sufficient (7), whereas AChR clustering likely requires TPR8 itself and the coiled coil motif extending beyond the last TPR (7). Accordingly, it is attractive to assume that CK2-dependent phosphorylation regulates AChR clustering at several levels among others by acting on Rapsyn and as previously shown on MuSK (1) (Table 2). In this context, it is remarkable that in patients with congenital myasthenic syndromes an insertion of a threonine amino-terminal to Ser-224 was reported (21) that might affect CK2-dependent phosphorylation of Ser-224 of Rapsyn. In fact, the prediction score for CK2-dependent Rapsyn Ser-224 phosphorylation changed from 0.81 to 0.69 by insertion of the additional threonine (KinasePhos 2.0).

Binding of Rac1 to CK2 is determined by Rac1 amino acid residues 28–47 (Fig. 3*c*). Only the first Switch domain of Rac1 is known to be located on this fragment between amino acid residues 30 and 40 (Fig. 3*a*). This and a second Switch domain flank the nucleotide binding site of Rac1. Previously, Rac1 was reported to be involved in Agrin-induced AChR cluster formation (10). Further investigation is required to understand the interaction between CK2 and the first Switch domain of Rac1 and its influence on AChR aggregation.

The importance of the phosphorylation of serine residues in consensus motifs was already reported in the regulation of 14-3-3 binding to target proteins (12). Consensus 14-3-3 recognition motifs such as R*S*X*S*X*P* and $RX_{1-2}SX_{2-3}S$ in which at least one of the serine residues is phosphorylated were identified in many 14-3-3 ligands (22, 23). Our pulldown data indicate binding of 14-3-3γ to CK2 by its amino acid residues 166–210 (Fig. 4*c*). Interestingly, in binding to CK2 it is serine residue 235 of 14-3-3γ that is phosphorylated (Fig. 5*d*). Serine residue 235 of 14-3-3γ is in close proximity to the epitope to which CK2 binds (Figs. 4*a* and 5*a*). It remains to be studied whether the interaction of CK2 is influenced by the phosphorylation status of serine residue 235 of 14-3-3γ.

Here, the most interesting finding might be the interaction between Dok-7 and CK2 because Dok-7 is also involved in human NMJ pathologies and is phosphorylated by CK2 at several serine residues (Fig. 8 and Table 1). Recessive inheritance of mutations in Dok-7 were shown to result in a defective structure of the neuromuscular junction and to be the cause of congenital myasthenic syndromes with proximal muscle weakness (24); and later, the mutations were shown to impair Dok-7 function (25). Recruitment of two adapter proteins, Crk and Crk-like, to the carboxyl-terminal domain of Dok-7 occurs after Agrin stimulates phosphorylation of two tyrosine residues (26). Obviously, it is the PH domain within the amino-terminal area of Dok-7 that is necessary and sufficient to bind CK2 (Fig. 6, *a* and *d*). This PH domain is mandatory for Dok-7 to activate MuSK (13). Nevertheless, how the PH domain contributes to activation of MuSK is unclear (13). The PH domain of Dok-7 is farther away, and it seems questionable whether Dok-7 phosphorylation of amino acid residues 238–347 interferes with Dok-7 PH/CK2 interaction. However, it is appealing to speculate that CK2 as a Dok-7 PH domain-interacting protein might also be important for activation of MuSK through Dok-7. MuSK itself was shown to be phosphorylated by CK2 (1). It might be challenging to differentiate the role of CK2 linked to MuSK or Dok-7 for AChR aggregation. A first step might be to overexpress the CK2-interacting epitope of Dok-7, its PH domain, in muscle cells to compete with the endogenous CK2/full-length Dok-7 interaction. This might result in lower CK2-dependent Dok-7 phosphorylation. It was reported that forced expression of Dok-7 induces aneural AChR clustering in C2 myotubes (13). Here, overexpression of phosphomimetic Dok-7 mutants was shown to induce aggregation of AChRs in C2C12 myotubes much more frequently than overexpression of wild type Dok-7 (Fig. 9*b*). The impact of these findings for

Dok-7 muscle pathology might be tremendous. Impaired Dok-7 function might then be compensated by modulated CK2 activity that is achievable by application of known drugs affecting CK2 (27).

Very recently, the Agrin-MuSK/Lrp4 signaling pathway was detected in hepatocellular carcinoma cells (28). An oncogenic role for Agrin was discovered, and it was found that Agrin enhances cellular proliferation (28). In this context it is worth mentioning that several years ago CK2 was reported to be involved in proliferative events in hepatocellular carcinoma cells (29). That CK2 might play a role in hepatocellular carcinoma cells similar to that at the NMJ, *i.e.* as a member of the interactome downstream of MuSK signaling, is an exciting tentative proposal.

Author Contributions—S. H. conceived and coordinated the study, designed the experiments, and wrote the paper. D. H. and M. S. designed, performed, and analyzed the experiments. S. H and D. H contributed to the preparation of the figures. All authors reviewed the results and approved the final version of the manuscript.

Acknowledgments—We are grateful to Dr. Olaf-Georg Issinger (Odense, Denmark) for providing us CK2-specific antibodies and Dr. Lorenzo A. Pinna (Universita Venetian Institute for Molecular Medicine, Padova, Italy) for personal communication on 14-3-3γ residues potentially phosphorylated by CK2.

References

1. Cheusova, T., Khan, M. A., Schubert, S. W., Gavin, A. C., Buchou, T., Jacob, G., Sticht, H., Allende, J., Boldyreff, B., Brenner, H. R., and Hashemolhosseini, S. (2006) Casein kinase 2-dependent serine phosphorylation of MuSK regulates acetylcholine receptor aggregation at the neuromuscular junction. *Genes Dev.* **20,** 1800–1816
2. Wu, H., Xiong, W. C., and Mei, L. (2010) To build a synapse: signaling pathways in neuromuscular junction assembly. *Development* **137,** 1017–1033
3. Meggio, F., and Pinna, L. A. (2003) One-thousand-and-one substrates of protein kinase CK2? *FASEB J.* **17,** 349–368
4. Sealock, R., Wray, B. E., and Froehner, S. C. (1984) Ultrastructural localization of the M_r 43,000 protein and the acetylcholine receptor in *Torpedo* postsynaptic membranes using monoclonal antibodies. *J. Cell Biol.* **98,** 2239–2244
5. Froehner, S. C., Luetje, C. W., Scotland, P. B., and Patrick, J. (1990) The postsynaptic 43K protein clusters muscle nicotinic acetylcholine receptors in *Xenopus* oocytes. *Neuron* **5,** 403–410
6. Gautam, M., Noakes, P. G., Mudd, J., Nichol, M., Chu, G. C., Sanes, J. R., and Merlie, J. P. (1995) Failure of postsynaptic specialization to develop at neuromuscular junctions of rapsyn-deficient mice. *Nature* **377,** 232–236
7. Colledge, M., and Froehner, S. C. (1998) To muster a cluster: anchoring neurotransmitter receptors at synapses. *Proc. Natl. Acad. Sci. U.S.A.* **95,** 3341–3343
8. Feng, G., Steinbach, J. H., and Sanes, J. R. (1998) Rapsyn clusters neuronal acetylcholine receptors but is inessential for formation of an interneuronal cholinergic synapse. *J. Neurosci.* **18,** 4166–4176
9. Moscoso, L. M., Merlie, J. P., and Sanes, J. R. (1995) N-CAM, 43K-rapsyn, and S-laminin mRNAs are concentrated at synaptic sites in muscle fibers. *Mol. Cell. Neurosci.* **6,** 80–89
10. Weston, C., Yee, B., Hod, E., and Prives, J. (2000) Agrin-induced acetylcholine receptor clustering is mediated by the small guanosine triphosphatases Rac and Cdc42. *J. Cell Biol.* **150,** 205–212
11. Willmann, R., and Fuhrer, C. (2002) Neuromuscular synaptogenesis: clustering of acetylcholine receptors revisited. *Cell. Mol. Life Sci.* **59,** 1296–1316
12. Strochlic, L., Cartaud, A., Mejat, A., Grailhe, R., Schaeffer, L., Changeux, J. P., and Cartaud, J. (2004) 14-3-3γ associates with muscle specific kinase and regulates synaptic gene transcription at vertebrate neuromuscular synapse. *Proc. Natl. Acad. Sci. U.S.A.* **101,** 18189–18194
13. Okada, K., Inoue, A., Okada, M., Murata, Y., Kakuta, S., Jigami, T., Kubo, S., Shiraishi, H., Eguchi, K., Motomura, M., Akiyama, T., Iwakura, Y., Higuchi, O., and Yamanashi, Y. (2006) The muscle protein Dok-7 is essential for neuromuscular synaptogenesis. *Science* **312,** 1802–1805
14. Wong, Y. H., Lee, T. Y., Liang, H. K., Huang, C. M., Wang, T. Y., Yang, Y. H., Chu, C. H., Huang, H. D., Ko, M. T., and Hwang, J. K. (2007) KinasePhos 2.0: a web server for identifying protein kinase-specific phosphorylation sites based on sequences and coupling patterns. *Nucleic Acids Res.* **35,** W588–W594
15. Willert, K., Brink, M., Wodarz, A., Varmus, H., and Nusse, R. (1997) Casein kinase 2 associates with and phosphorylates dishevelled. *EMBO J.* **16,** 3089–3096
16. Luo, Z. G., Wang, Q., Zhou, J. Z., Wang, J., Luo, Z., Liu, M., He, X., Wynshaw-Boris, A., Xiong, W. C., Lu, B., and Mei, L. (2002) Regulation of AChR clustering by Dishevelled interacting with MuSK and PAK1. *Neuron* **35,** 489–505
17. Nghiêm, H. O., Bettendorff, L., and Changeux, J. P. (2000) Specific phosphorylation of *Torpedo* 43K rapsyn by endogenous kinase(s) with thiamine triphosphate as the phosphate donor. *FASEB J.* **14,** 543–554
18. Schwarz, J., Proff, J., Hävemeier, A., Ladwein, M., Rottner, K., Barlag, B., Pich, A., Tatge, H., Just, I., and Gerhard, R. (2012) Serine-71 phosphorylation of Rac1 modulates downstream signaling. *PLoS One* **7,** e44358
19. Boekhorst, J., van Breukelen, B., Heck, A., Jr., and Snel, B. (2008) Comparative phosphoproteomics reveals evolutionary and functional conservation of phosphorylation across eukaryotes. *Genome Biol.* **9,** R144
20. Shiromizu, T., Adachi, J., Watanabe, S., Murakami, T., Kuga, T., Muraoka, S., and Tomonaga, T. (2013) Identification of missing proteins in the neXtProt database and unregistered phosphopeptides in the PhosphoSitePlus database as part of the Chromosome-centric Human Proteome Project. *J. Proteome Res.* **12,** 2414–2421
21. Leshinsky-Silver, E., Shapira, D., Yosovitz, K., Ginsberg, M., Lerman-Sagie, T., and Lev, D. (2012) A novel mutation in the TPR6 domain of the RAPSN gene associated with congenital myasthenic syndrome. *J. Neurol. Sci.* **316,** 112–115
22. Fu, H., Xia, K., Pallas, D. C., Cui, C., Conroy, K., Narsimhan, R. P., Mamon, H., Collier, R. J., and Roberts, T. M. (1994) Interaction of the protein kinase Raf-1 with 14-3-3 proteins. *Science* **266,** 126–129
23. Muslin, A. J., Tanner, J. W., Allen, P. M., and Shaw, A. S. (1996) Interaction of 14-3-3 with signaling proteins is mediated by the recognition of phosphoserine. *Cell* **84,** 889–897
24. Beeson, D., Higuchi, O., Palace, J., Cossins, J., Spearman, H., Maxwell, S., Newsom-Davis, J., Burke, G., Fawcett, P., Motomura, M., Müller, J. S., Lochmüller, H., Slater, C., Vincent, A., and Yamanashi, Y. (2006) Dok-7 mutations underlie a neuromuscular junction synaptopathy. *Science* **313,** 1975–1978
25. Hamuro, J., Higuchi, O., Okada, K., Ueno, M., Iemura, S., Natsume, T., Spearman, H., Beeson, D., and Yamanashi, Y. (2008) Mutations causing DOK7 congenital myasthenia ablate functional motifs in DOK-7. *J. Biol. Chem.* **283,** 5518–5524
26. Hallock, P. T., Xu, C. F., Park, T. J., Neubert, T. A., Curran, T., and Burden, S. J. (2010) Dok-7 regulates neuromuscular synapse formation by recruiting Crk and Crk-L. *Genes Dev.* **24,** 2451–2461
27. Cozza, G., Pinna, L. A., and Moro, S. (2013) Kinase Ck2 inhibition: an update. *Curr. Med. Chem.* **20,** 671–693
28. Chakraborty, S., Lakshmanan, M., Swa, H. L., Chen, J., Zhang, X., Ong, Y. S., Loo, L. S., Akıncılar, S. C., Gunaratne, J., Tergaonkar, V., Hui, K. M., and Hong, W. (2015) An oncogenic role of Agrin in regulating focal adhesion integrity in hepatocellular carcinoma. *Nat. Commun.* **6,** 6184
29. Sass, G., Buerbank, S., Klinger, N., Ocker, M., Cheusova, T., Hashemolhosseini, S., Papadopoulos, T., and Tiegs, G. (2008) CK2 contributes to cell survival in hepatocellular carcinoma by activating NFκB and contributing to the WNT signal transduction pathway. *Journal of Hepatology* **48,** Suppl. 2, S135–S136
30. Frail, D. E., McLaughlin, L. L., Mudd, J., and Merlie, J. P. (1988) Identification of the mouse muscle 43,000-dalton acetylcholine receptor-associated protein (RAPsyn) by cDNA cloning. *J. Biol. Chem.* **263,** 15602–15607